How color language is shaped by the variability of reflected light under changes of illumination

Christoph Witzel, François Cinotti and **J. Kevin O'Regan**[1]

Abstract. The relationship between the sensory signal of the photoreceptors and the language of color is completely unclear. A recent finding established a surprisingly accurate correlation between color terms and so-called singularities in the laws governing how sensory signals for different surfaces change across illuminations. The sensory signal depends on the reflectances of the surfaces, the illuminants, and the sensitivity profiles of the human photoreceptors. This paper examines the role played by reflectances, illuminants and cone sensitivities in determining the relationship between color terms and the singularities in laws of the sensory change. We found that this relationship holds for a wide range of illuminants, as long as these are predominantly broad-band. The relationship also exists when using sensors that differ in important aspects from human photoreceptors, as long as these sensors cover the whole visual spectrum. According to our results, the characteristics of the reflectance spectra are the key factor that determines the relationship between the color terms and the sensory singularities.

1 INTRODUCTION

Which are the sensory characteristics of color vision that determine color language? This is an intriguing question because the relationship between the sensory characteristics of color vision and the color terms used to communicate color is a major, unresolved question. Answers to this question may elucidate the understanding of color vision as well as the general relationship between perception and language.

1.1 Background and relevance

Colors are communicated through color terms, such as *red*, *pink* and *purple*. These color terms categorize the multitude of perceivable colors into groups, the color categories. While color terms differ, the corresponding categories share some statistical regularities across languages [1-3]. The prototypes of red, yellow, green, and blue are particularly stable across languages [4, 5]. Since the prototypes of the categories are representative for the whole category, they are also called *focal colors*. However, the origin of color categories as well as their relationship to color perception remain unknown [6], in particular since color perception does not reflect the linguistic categories, at least not at a sensory level [7].

The sensory characteristics of human color vision are first and foremost defined by the activation of the 3 photoreceptors, the cones. Each cone is particularly sensitive in a specific region of the visible spectrum of light. Since one cone is particularly sensitive to comparatively short, one to comparatively long wavelengths, and one to wavelengths in between, they are called short-, middle-, and long-wavelength cones, or S-, M-, and L-cones. The combined excitation of these 3 cones carries the information about wavelength differences, and hence the color signal. To refer to a triad of cone excitations the term *LMS signal* will be used here. Further low-level stages of color processing are known, but the link to the ultimate appearance of colors and to color categorization remains a major question of color research [e.g. 8].

A new approach proposed by Philipona & O'Regan [9] discovered a property of the LMS signal that is strongly related to focal colors. This approach did not examine how a particular LMS signal is processed in the visual system. Instead, it inspected how the variation of LMS signals is constrained by the relationship between the human cones and the visual environment.

The LMS signal is determined by the excitation of the cones through the light that impinges on the retina, the *impinging light*. More precisely, it depends on the wavelength composition (here *spectrum*) of the impinging light (henceforth *impinging spectrum*). Impinging light can come directly from a light source (*emitted light*), or it can be reflected off a surface (*reflected light*). In the latter, the impinging spectrum is the linear combination of *the* spectrum of the illumination, i.e. the *illuminant*, and the spectral reflectance properties of the surface, the *reflectance spectra*. The LMS signal can be determined by applying the sensitivities of the human photoreceptors (*cone fundamentals*) to the impinging spectrum.

When the illumination changes, the reflected spectrum changes. Since the reflected light corresponds to impinging light for a given surface, the change of the reflected spectrum implies a change of the LMS signal.

That new approach discovered that the way in which the LMS signal changes across a wide range of illuminations is particular for the focal colors that correspond to red, yellow, green, and blue.

To be more precise, Philipona and O'Regan noticed that in a mathematical sense, surfaces with focal colors were "singular", in that the dimensionality of the variation in reflected light was reduced as compared to other surfaces. This finding implies that the color categories used in communication organize around colors that correspond to surfaces that have particular properties under changing illuminations. In the natural environment illuminations change mostly slowly by themselves, such as daylight from dawn to dusk. However, fast changes occur when the observer moves the surfaces, e.g. from shadow to sunlight or under a canopy of trees. They also happen when the observer tilts a surface under different simultaneous illuminations. Hence, those properties that relate

[1] Laboratoire Psychologie der Perception, Université Paris Descartes, email: cwitzel@daad-alumni.de

surfaces to color categories are mainly present when the observer interacts with objects so as to perceive their surfaces across different illuminations. According to this approach, color language originates through the observer's interaction with the visual environment. The visual environment and the sensitivity of human photoreceptors have a certain stability across cultures and languages. Hence, this finding also explains why the focal colors of red, yellow, green, and blue are particularly stable across languages.

1.2 Objective

However, the previous studies [9, 10] that provided evidence for this relationship between changes in the sensory signal and focal colors, employed particular kinds of illuminants, surfaces, and human photoreceptors to establish the observed patterns. More precisely, they used natural illuminants and a limited set of standard color chips (*Munsell chips*) with particular properties (maximal saturation). As we will explain in detail in the respective sections below, those illuminants, reflectance spectra, and the human sensors have particular properties that might be responsible for the relationship between the changes of the LMS-signal and the focal colors.

The present study investigates whether that relationship between LMS signal and focal colors is due to the characteristics of the illuminations, the reflectances, or the sensors. For this purpose, we examine this relationship, first, when using fluorescent and random illuminants, second, when applying sensors with spectral sensitivities other than the human photopigments, and third, different sets of reflectance spectra that result in similar colors as Munsell chips under neutral illumination.

2 GENERAL METHOD

The results of Philippona and O'Regan [9] about the relationship between changes of the LMS signal and focal colors were the reference for all our comparisons. For this reason, we used the same algorithms (i.e. Matlab programs) for all calculations, and the same illuminants, refeflectances, and sensors as a reference to evaluate how strongly the relationship between LMS signal and focal colors changes when using different illuminants, reflectances, and sensors, respectively.

2.1 Mathematical approach

Philipona and O'Regan's [9] approach consists of three observations.

2.1.1 Relationships between LMS signals

The first observation concerns the relationship between the LMS signal of the illuminations (*illuminant signal*) and the LMS signal of the light reflected from the surfaces (*reflection signal*) across those illuminations. The illuminant signal is the LMS signal that would result if the light of the illumination directly fell into the eye, that is, without being reflected by a surface. The reflection signal for a surface is the LMS signal that results when light from the illuminant is reflected off the surface. The colour of a surface is thus seen as a map that transforms an incoming illuminant LMS signal, into an outgoing reflection LMS signal.

A priori, the maps that link illuminant LMS signals to reflection LMS signals could be arbitrary, taking illuminant LMS triples into arbitrary reflection LMS triples. But what Philipona & O'Regan (2006) observed was the surprising result that for most surfaces, the maps were very accurately linear. The linear transformation between the illuminant (iLMS) and reflection signals (rLMS) may be characterized by a 3 x 3 *transformation matrix* A that converts the illuminant signal into the reflection signals of a given surface across all illuminants. The matrix A that does this with minimum error (maximum variance explained) can be obtained by linear regression. Philipona and O'Regan showed that the residual variation that is not explained through the linear transformation is almost zero (no more than around 0.015 of the total variance) for each of the reflectances.

Hence, reflection signals of a given surface across a wide range of illuminations may be approximated with almost perfect accuracy by a linear transformation of the LMS signal of those illuminations. The matrix A that accomplishes the linear transformations is specific to a given surface reflectance.

2.1.2 Sensory singularities

The second observation concerns the properties of the matrix A that defines the linear transformation. The 3 cone excitations that make up the LMS illuminant and reflection signals may be represented in a three-dimensional space, the cone-excitation space. In general, a 3 x 3 matrix will take a point in three-dimensional space, and project it into another point in three dimensional space. For a typical matrix A, when the illuminant varies over the whole cone excitation space, the reflected LMS signal will also be able to vary across the whole cone-excitation space. However, sometimes a matrix will take points in three dimensional space and project them into a two-dimensional, or one-dimensional subspace of three dimensional cone excitation space. Such matrices are called *singular* matrices. Surfaces corresponding to matrices A that are singular have the property that the reflection signal will be restricted to a plane or a line within the three-dimensional cone-excitation space. The degree to which this happens is measured by the *singular values* of the matrix, as calculated by the *singular value decomposition* of the matrix. When a singular value is near to zero, there is an axis along which the variation of the reflection signal will be very small. Illuminant signals transformed by matrices with one near-zero singular value are projected into reflected signals restricted to a plane in cone excitation space. When two singular values are close to zero, there are two axes along which the variation of the reflection signal is small. Illuminant signals transformed by matrices with two near-zero singular values are projected into reflected signals restricted to a line in cone excitation space.

Singularities and focal colors

The third observation consists in a relationship between the singularity and focal colors. In order to compare singularities of the matrices corresponding to different surfaces an index was needed to assess the singularity of a transformation matrix A with a single number. As a result, the last value is closest to zero among all values. If this value is negligibly small compare to the other two values, the ratio between the second largest value and this last value will be large because the denominator is comparatively close to zero. However, if two values are close to zero, then the ratio between the first and the second value will be large, because only

the first value is high, while the second value would be comparatively close to zero. As a result, the ratio between the first and the second largest singular values indicates whether the two dimensions are negligible and the transformation through matrix A is approximately one-dimensional. If this is not the case, the ratio between the second and third shows whether the one dimension is negligible and the transformation is approximately two-dimensional.

Philippona and O'Regan decided not to make a difference between cases when the reflectance signal was restricted to a one- or a two-dimensional subspace of cone excitation space. Instead they focused on whether the reflectance signal could occupy a three-dimensional region or not. They defined a singularity index in the following way. They sorted the three singular values in decreasing order (similar to what is done in a principal component analysis). They took the ratio of the first to the second of the sorted singular values (which will be large if there are two small singular values), and the ratio of the second to the third of the sorted singular values (which will be large if there is one small singular value). The maximum of the two ratios gives an indication of the degree to which the matrix compresses incoming illuminant signal into either a two-dimensional or a one-dimensional subspace of three-dimensional cone excitation space. The higher this singularity index, the less three-dimensional is the space occupied by the illuminant signal in cone excitation space.

This singularity index allows comparing singularities across the reflectances. The singularities for the Munsell chips are illustrated by Figure 3.c.

By visual inspection, Philippona and O'Regan [9] observed that the pattern of singularities across Munsell chips (Figure 3.c) looked similar to the pattern of relative frequencies of focal color choices across those Munsell chips (Figure 3.b). In particular, high singularity indexes coincided with reflectances that are chosen most often and corresponded to focal red, yellow, green, and blue in English.

2.2 Spectra

As in Philippona and O'Regan [9], all spectra were normalized so that their maximum corresponds to 1.

2.2.1 Illuminants

Philipona and O'Regan [9] as well as Vazquez-Corral and colleagues [10] used measured and simulated daylight illuminants. As measured illuminants, they took 99 measurements of daylight spectra in Granda [11], and 238 daylight spectra of forests in Maryland [12]. The simulated daylight illuminants were based on the 3 basis functions specified by Judd and colleagues [13]. The parameters that combine these basis functions were fixed so that the resulting spectra produce a chromaticities within the area span by D45, D65, and D85. Examples of these illuminants are shown in Figure 1.a.

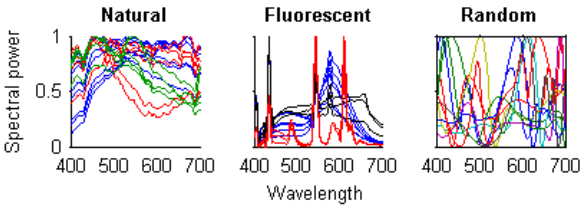

Figure 1. Illuminants. Panel a.) Examples of daylight illuminants with red curves corresponding to 5 examples from the Grenada data base, green curves to the Maryland-forest illuminants, and blue curves to the simulated daylight spectra. Panel b.) shows the 12 illuminants F, where the blue curves correspond to the semi-broadbent illuminants F_{1-6}, the black curves to the broadbent illuminants F_{7-9}, and the red curves to the narrow, triband illuminant F_{10-12}. Panel c.) illustrates 10 examples of random spline spectra.

2.2.2 Photoreceptors

In order to represent the sensitivity of the human photoreceptors, Philippona and O'Regan [9] applied 10-deg Stiles and Burch Color-Matching Functions [14], and Vazquez-Corral and colleagues [10] used the cone-fundamentals of Smith and Pokorny [15]. We employed the Stockman-Sharpe cone fundamentals of [16] for the simple reason that they directly refer to the sensitivity of the human photoreceptors and are particularly precise. In any case, results do not depend on whether cone fundamentals or color matching functions are applied (for details see SENSORS). The cone fundamentals are illustrated by Figure 2.a.

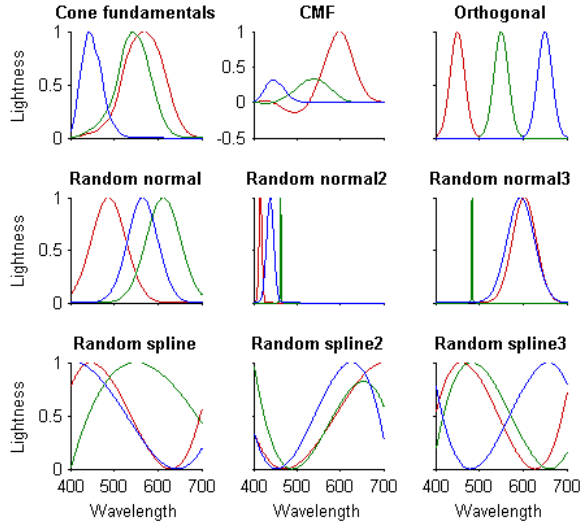

Figure 2. Real and artificial sensors. Panel a.) shows the cone fundamentals of Stockman and Sharpe [16], b.) the color matching functions of Stiles and Burch [14], c.) non-overlapping, orthogonal sensors, d-f) spectra consisting of random normal distributions, and g-i) random spline spectra.

2.2.3 Reflectances

The reflectances for glossy Munsell chips were retrieved from the data base of the University of Joensuu [17]. To establish the relationship between singularities and focal colors the reflectance spectra of a set of 320 maximally saturated Munsell chips (i.e. maximum *Munsell Chroma*) were used. The Munsell System arranges color chips by their hue (Munsell Hue), lightness (Munsell Value), and chroma (Munsell Chroma) [18]. The Munsell

chips varied in 40 levels of hue and 8 levels of lightness (Munsell Value 2 to 9). Throughout this paper, the set of Munsell chips is arranged vertically by its 8 lightness and horizontally by its 40 hue levels. Figure 3.a illustrates the variation of Munsell Chroma across the 8 times 40 chips.

This choice of Munsell chips allows to compare the singularities of these reflectances with the focal colors measured in the *World Color Survey*, a cross cultural study on color naming [4]. Figure 3.b shows the relative frequency by which observers of 110 non-industrialised societies chose focal colors. These modes of these choices coincide with the prototypes of red, yellow, green and blue in English.

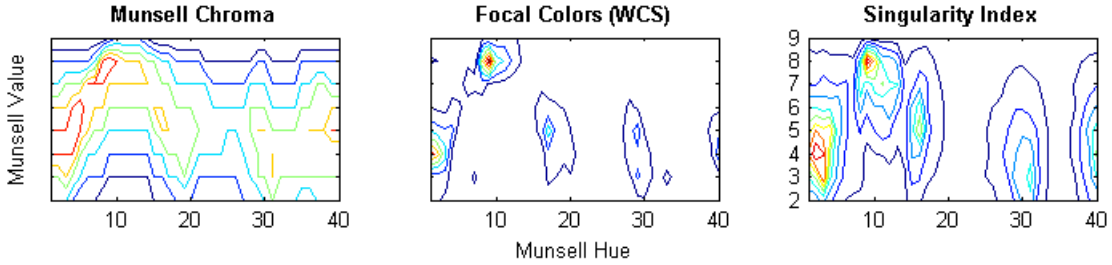

Figure 3. Results for the Munsell chips used by Philipona and O'Regan [9]. Graphics show Munsell chips arranged by their hue (x-axis) and lightness (y-axis), which are defined as Munsell Hue and Munsell Value in the Munsell Color System [18]. In panel a contours refer to the singularity indices, in panel b to the relative frequencies of focal color choices in the World Color Survey (WCS [4]), and in panel c to Munsell Chroma. Red contours correspond to high, green to medium, and blue to low values.

2.3 Analyses

To evaluate the impact of changes to the settings (illuminants, reflectances, or sensors) on the pattern of singularities, we compared singularities for new settings (e.g. random illuminants) to the singularities that resulted from Philipona and O'Regan's [9] settings (Figure 3.c). In order to quantify and to statistically evaluate the similarity between the patterns of singularities, we calculated correlations across the 320 Munsell chips.

In order to assess the relationship between singularities and focal color choices we calculated the correlation between the relative frequencies of focal color choices and the singularities across Munsell chips. For Philippona and O'Regan's [9] settings, singularities explained 42% of the variance of focal color choices (Figure 3.b) ($r=0.65$, $p<0.0001$). This correlation quantifies the similarity between the patterns in panels b and c of Figure 3.

3 ILLUMINATION

As explained by Philipona and O'Regan [9], the effect of the spectra that may be decomposed into 3 basis functions can necessarily modeled by a three-dimensional transformation. The first question is, whether this transformation is as perfect as reported in figure 1 of Philipona and O'Regan [9] when using illuminants that may not be decomposed into 3 basis functions. The second, main question is whether the same distribution of singularities are reproduced with these artificial illuminants, as those obtained with the natural ones.

3.1 Method

To test for the role of the distribution of illuminants, we inspected what happens to the singularity index, when using different kinds of artificial illuminants that cannot be decomposed into 3 basis functions. For this purpose, we used a set of 12 standard illuminants $F_{1\text{-}12}$, which simulate fluorescent lights. The spectra are displayed in figure Figure 1.b. And we used a set of 100 random illuminants that were produced as follows: For each random spectrum, 10 data points (x = wavelength, y = relative intensity) were randomly created within the visual spectrum, i.e. between 400 and 700nm. A random value along the y-axis (intensity) was determined at the beginning and end of the spectrum. A smooth curve was interpolated through cubic splines. The values at the beginning and end of the spectrum prevented that intensities systematically increase at the beginning and end of the spectrum, since cubic functions increase to positive or negative infinity. 10 example random spectra are shown in figure Figure 1.c. Apart from that Stockman-Sharpe cone fundamentals and maximally saturated Munsell chips were used as in Philippona and O'Regan [9].

3.2 Results

For all sets of illuminations, reflected signal calculated through the transformation matrices A were extremely similar to the actual reflected signal based on the convolution of spectra. The mean variance explained by the linear calculation with transformation matrix A was above 99% for fluorescent ($R^2=0.998$) and random spline illuminants ($R^2=0.997$). This was almost as high as for natural illuminants ($R^2=99985$). This result indicates that the reflected signal can be approximated with high accuracy for fluorescent and random spline illuminants, too.

The singularity indices for natural illuminants and random illuminants were highly correlated across the 320 Munsell chips ($r=0.89$; $p<0.001$). Fluorescent illuminants yielded much lower, but still significant correlations with the SI of natural ($r=0.36$, $p<0.001$) and random spline illuminants ($r = 0.48$, both $p < 0.0001$). These results imply that random spline illuminants produced similar singularities across Munsell chips as natural illuminants, but singularities calculated for fluorescent lights differed from both.

Since the singularities calculated for the transformations under random spline illuminants were similar to the one under natural illuminants, they also explained 32% of the variance of the focal color choices ($r = 0.56$, $p < 0.001$). In contrast, singularities for fluorescent illuminations explained only 8% of the variance of

focal colors (r=0.29, p<0.001). According to these results, the relationship between singularities and focal colors is slightly affected when using random instead of natural illuminants. Using fluorescent illuminants undermines this relationship.

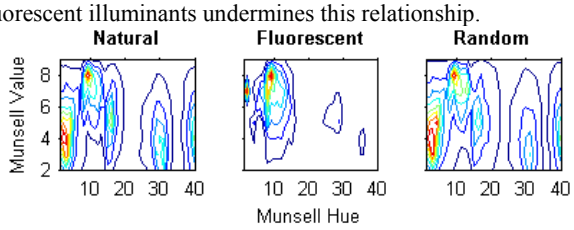

Figure 4. Singularity indices for different types of illuminants. Panel a.) Natural illuminants of Philippona and O'Regan [9]; panel b.) Fluorescent illuminants; panel c) Random spline illuminants. Format as in Figure 3.c.

3.3 Discussion

While random spectra produced similar singularities as natural illuminants, singularities for fluorescent illuminants differed from both. Moreover, the correlation between singularities and focal colors is also much lower for fluorescent than for the other illuminants. A particularity of fluorescent spectra is that they have a few pronounced peaks in their spectral power distributions (cf. Figure 1.b). Hence, they have rather narrow-band spectra compared to natural illuminants. It might be that this peakiness is the reason for the particularity of the singularity indices for fluorescent lights. Hence, the bandwidth of illuminants may play an important role for the relationship between singularities and focal colors.

However, random spline illuminants also include both very narrow-band, peaky and broad-band spectra (cf. Figure 1.c). The observation that random spline illuminations produced a similar singularity pattern as the one found with natural illuminants strongly indicates that the type of illumination is not the major source of variation of singularities across colors – as long as they are predominantly broadband.

In the natural environment most illuminations are produced by filtered and scattered daylight. As mentioned above, daylight may be approximated by 3 basis functions [13], and is predominantly broad-band (Figure 1.a). As a result, most illuminants in the natural environment should be predominantly broadband, if not strong filtering occurs. For this reason, the relationship between singularities and focal colors most probably holds in the natural visual environment.

4 SENSORS

The color signal may be mathematically represented by color matching functions for arbitrary, virtual RGB sensors, Tristimulus values (XYZ) and cone fundamentally (LMS). The Stockman-Sharpe cone fundamentals and the Stiles Burch color matching functions are illustrated in Figure 2.a-b. The singularity index is largely invariant as to this kind of representation. This is illustrated by the Sis in Figure 5.a-b, respectively. These SIs correlate with r = 0.999 across Munsell chips. The tiny deviations of SIs between the two sensors are probably due to differences in the empirical measurements that underlie the respective color matching functions. Koenderinck [19] argued that the constraints of the cone sensitivities may be at the source of invariances in the distribution of object colors. We tested this idea by using artificial sensors.

4.1 Method

To check whether the correlations between the spectral sensitivities affects the singularity index, we produced three equally spaced spectral sensitivities that do not overlap (Figure 2.c). This was done through three normal distributions that were distanced by 6 standard deviations, so that less than 0.3% overlap, and the overlapping 0.3% were set to zero. Then we produced 3 random Gaussian spectral sensitivity functions that could overlap, but would converge towards zero within the visible spectrum. The peaks of each function in terms of wavelenghts as well as their respective width (standard deviations) were determined randomly (Figure 2.d-f). And finally, we produced 3 random spectral sensitivities based on cubic spline interpolations (Figure 2.g-i). These overlapped and did not converge towards 0. To test the impact of the sensors on the SI, the original Munsell chips and natural illuminations were used as illuminants and reflectances here as in Philipona and O'Regan [9].

4.2 Results

Panels c-i of Figure 5 show the distribution of the singularity index when using artificial sensors. Orthogonal, non-overlapping sensors (Figure 5.c) produced extremely similar singularity indices as Stockman-Sharpe cone fundamentals (Figure 5.a), and Stiles-Burch color matching functions (Figure 5.b). In fact, SIs based on the orthogonal sensors correlated with r = 0.97 and 0.96 the SI for the human photopigments as measured by Stockman-Sharpe and Stiles-Burch, respectively. Given the high similarity in singularities, it is no wonder that the SIs of orthogonal sensors yielded correlations (r=0.62, p<0.001) with the focal colors that were almost as high as those for the human photoreceptors (both r = 0.65). These results show that the overlaps among spectral sensitivities and the resulting correlations among the color signals are irrelevant for the distribution of the singularity index across colors, and their relationship to focal colors.

The singularities for the random normal sensors in panels d and f were also highly correlated with the singularities of the photoreceptors (r=0.87 and r=0.91) and the focal colors (r=0.57 and r=0.63). However, the random normal distribution in Figure 1.e did not yield a significant correlation with the singularities for the photopigmens (r=-0.05, p=0.38) and the focal colors (r=0.03, p=0.60).

Singularity indices with random spline sensors (last row, panels g-i) were correlated with those of the photopigments (r = 0.59, r = 0.66, and r = 0.78, respectively, all p < 0.0001). Moreover, they yielded correlations with the focal colors r=0.37, r=0.31, r=0.50, respectively, all p<0.001), explaining 14%, 10% and 25% of the variance.

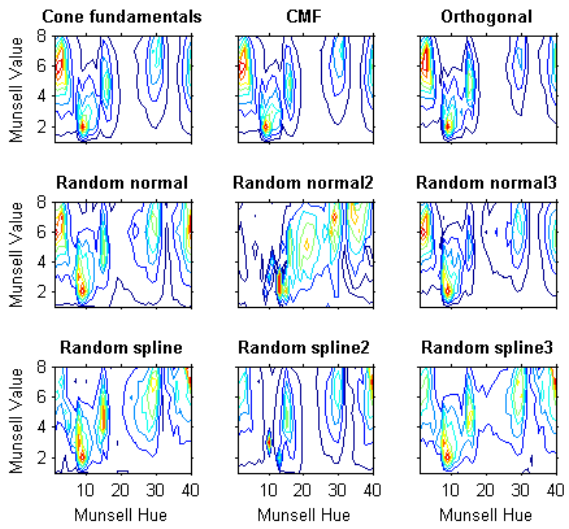

Figure 5. Singularity Indices for different sensors. a.) cone fundamentals of Stockman Sharpe; b.) color matching functions (CMF) of Stiles and Burch; c.) orthogonal sensors. Format as in Figure 1.c.

4.3 Discussion

In sum, singularities were surprisingly stable across different sensors. The fact that they barely changed when using orthogonal sensors instead of photopigments illustrates that the correlation of L- and M-cones (red and green curve in Figure 2.c) does not play any role for the distribution of singularities across the color chips, and their relationship to focal colors.

In contrast the random normal spectra in Figure 2.d all overlap strongly, and in Figure 2.f one of the sensors is extremely narrow-band. The observation that these sensors yield similar singularities as the photopigments suggests that it does not matter whether the sensitivity spectra overlap, or whether some of the sensors have extremely narrow-band spectra. The fact that even the singularities for the random spline sensors yield considerable correlations with those of the photopigments and even with the focal colors implies that the shape of the sensitivity functions is not a major factor either.

In contrast to all the other sensors, the random normal sensors in Figure 2.e did not yield such correlations. The sensors do not cover the whole visual visible. Additional analyses with more randomly generated normal and spline sensors showed that sensors that do not cover the whole visible result in much lower correlations with the singularities of the photopigments and the focal color choices. These observations suggest that the main characteristic of the sensors that matters for the relationship between singularities and focal colors is whether their spectra are distributed over the whole visible spectrum or not.

5 SURFACES

There are 2 critical questions concerning the surfaces. First, the maximally saturated Munsell chips used by Philippona and O'Regan [9] to establish a relationship with focal colors had different Munsell Chroma because the Munsell system does not provide the same range of Chroma for all chips. In fact, their singularity index correlated as much (or even more) with Munsell Chroma ($r=0.70$, $p<0.0001$) as with focal color choices ($r=0.65$, $p<0.0001$). At the same time, it has been observed that focal color choices also coincide with the most saturated Munsell chips [20, 21]. In fact, focal color choices correlate with Munsell Chroma ($r=0.41$, $p<0.0001$). Consequently, the question arises of whether the singularity index is related to Chroma, and whether the relationship between singularity index and focal colors is due to the differences in Chroma of the chips. To test this idea, we examined Munsell chips that are more uniform in chroma.

Second, the reflectance properties of Munsell chips may be particular because they are made out of particular artificial pigments. The question arises of whether surfaces that look the same or at least highly similar under the most common illuminations produce similar singularities. For example, does a surface with the same red as the perfectly red Munsell chip, but with a different reflectance spectrum also have a particularly high singularity? To investigate this question we examined surfaces that produce the same LMS signal when they reflect white light. When light produces exactly the same LMS signal, it is called *metameric*. While it is true that these surfaces will not be metameric under different illuminations, they look still similar under a wide range of neutral illuminations, i.e. a red surface would still be red under daylight and a tungsten bulb (whether this is due to color constancy or insensitivity to small changes is not of importance here). However, in order to assess potential differences resulting from small changes in illumination, we used two kinds of light, white light and daylight.

5.1 Method

In order to make Munsell chips more uniform in chroma, we simply replaced all Munsell chips with a Munsell Chroma above 6 in the set of maximally saturated Munsell chips by chips with a Munsell Chroma equal to 6. However, some particularly light or dark Munsell chips (Munsell Value = 2 or 9) are not available at this Munsell Chroma. Hence, even our set of Munsell chips with uniform Munsell Chroma still involved differences in Munsell Chroma across Munsell chips. This was barely avoidable since some dark and light colors were only available with a Munsell Chroma of 2, and at this level of chroma all colors tend to be called "grey". Hence, it would be meaningless to compare such desaturated colors to focal color choices. For the sake of simplicity, we will call these chips "uniformly saturated" for now, and come back to this issue when discussing results.

To obtain sets of reflectances that are metameric with the Munsell chips under neutral illuminations, we determined surface reflectances that produce metameric LMS signals, when reflecting equal energy white or daylight. For this purpose, we calculated the spectra reflected off the surfaces of the Munsell chips under equal energy light (CIE standard illuminant E) and simulated daylight (CIE standard illuminant d65). Then we calculated the *fundamental metamers* for the spectra of the scattered light [22]. A fundamental metamer is the part of the impinging spectrum that is common to all metameric impinging spectra. Finally, we determined the reflectances that would reflect these lights under those illuminants (Note that for illuminant E the fundamental metamer for the impinging spectra are the same as calculating the fundamental metamer directly for the surface reflectance). This provides us with two sets of surfaces for each set of Munsell chips (maximally and

uniformly saturated), namely one that reflects metameric light under illuminant E, and one that reflects such light under illuminant d65.

As before, the set of natural illuminants and the human cone fundamentals were used to calculate LMS signals and singularity indices.

5.2 Results

More uniform Munsell Chroma (Figure 6.b) changed the distribution of singularity indices as compared to the maximally saturated Munsell chips (panel a). However, the correlation between both sets of singularity indices explained only 30% of the variance; however, it was still significant, indicating that some similarities between the two distributions ($r=0.55$, $p<0.001$). There is no data available for focal color choices of uniformly saturated Munsell chips. These chips are never chosen as focal colors for red, yellow, green, and blue, but they might be chosen for brown and pink. At the same time, the singularity indices of these chips are barely correlated to the focal color choices for the maximally saturated chips ($r=0.14$, $p<0.01$). These results indicate that the singularities of the surfaces are strongly related to saturation and chroma. Moreover, changes in chroma affect the relationship between focal colors and singularities.

Using fundamental metamers also affected the patterns of singularities across colors (second and third row compared to first row in Figure 6). The singularities for the fundamental metamers of the maximally saturated Munsell chips under illuminant E (panel c) and D65 (panel e) were still fairly similar to those of the real Munsell chips (panel a). Correlations between the singularity indices of the original chips and the ones of the fundamental metamers under illuminant E and D65 explained 60% ($r=0.77$, $p<0.001$) and 33% of the variance ($r=0.57$, $p<0.001$), respectively. Moreover, the SIs of the fundamental metamers under illuminant E and D65 explained 21% ($r=0.46$, $p<0.001$) and 10% of the focal color choices ($r=0.32$, $p<0.001$).

The pattern of singularities was still more different between the uniform Munsell chips (panel b) and their fundamental metamers (panels d and f). There correlations explained only 12% for the metamer under illuminant E ($r=0.35$, $p<0.001$) and 10% for the metamer under D65 ($r=0.32$, $p<0.001$). These results show that the pattern of similarities is not the same across surfaces that are metameric under white light and natural daylight.

Finally, the singularity indices for these fundamental metamers of the uniformly saturated chips barely correlated with the singularity indices of the original maximally saturated chips (panel a) ($r=0.07$, $p<0.21$; $r=0.11$, $p<0.06$) and not correlated with the focal color choices ($r=-0.11$, $p=0.06$; $r=-0.07$, $p=0.24$). Only the results for the fundamental metamers under the two kinds of illuminants were almost the same for maximally (panel c and e; $r=0.92$), and uniformly saturated Munsell chips (panel d and f, $r=0.95$). The high similarity between the singularities for the two kinds of fundamental metamers is not surprising since illuminant E and D65 are very similar. While illuminant E is maximally broadband (equal energy), D65 is also a broadband spectrum. Consequently, the LMS signals of the same surfaces will be very similar under these illuminants, and as a consequence singularity indices must be similar.

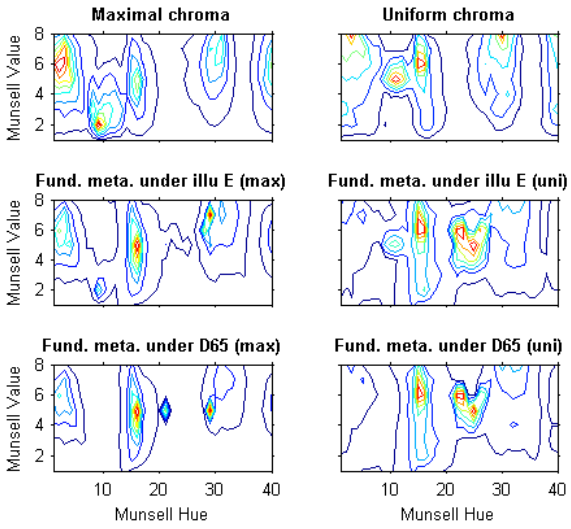

Figure 6. Singularity index for real and artificial Munsell chips. The panels on the left and right sides, respectively, correspond to Munsell chips with maximal and uniform Munsell Chrom. The first row (panels a-b) corresponds to the original reflectance spectra of the Munsell chips, the second row (panels c-d) to the reflecatances that reflect lights that are metameric with the Munsell chips under illuminant E, and the third row (panel e-f) to reflectances that reflect metameric lights under illumination D65.

5.3 Discussion

In sum, results with different levels of Munsell Chroma show that the singularity index and its relationship to focal colors depends on chroma. However, it must be kept in mind that even our set with uniform Munsell Chroma did not result in the same Munsell Chroma for all Munsell chips. Moreover, Munsell Chroma is not a reliable control for perceived chroma in the first place [23, 24], i.e. even if Munsell Chroma was the same across chips this would not mean that the actual perceived chroma would be perfectly equal. Given the relationship between singularities and chroma, inequalities in chroma may explain some of the small, but significant correlations between singularity indices across all the reflectances tested here, i.e. including the ones in the set with uniform chroma. The results with fundamental metamers show that not all surfaces that look like the typical red, yellow, green, or blue yield particularly high singularity indices.

These findings suggest that there is something particular about the reflectances of Munsell chips that produces the strong relationship between singularities and focal colors. For example, it might be that pigments are particularly pure for the chips that correspond to focal colors. In this case, these chips would have reflectances with narrower bandwidth. These narrow bandwidths might be the origin of both, highest ranges of available chroma in the Munsell system, and pronounced singularities.

6 CONCLUSION

The present study investigated whether characteristics of illuminants, reflectances, or sensors are the main determinants of the relationship between focal colors and the singularities in the variation of LMS signals across changes in illumination. We found

that the relationship between singularities and focal colors is stable across a wide range of illuminations, including random illuminations, as long as they are predominantly broadband. It is also stable across variations of the sensors as long as the sensitivities of these sensors cover the whole range of the visual spectrum. In contrast, the characteristics of the reflectances strongly affected the distribution of singularities across colors, and hence was crucial for the relationship between singularities and focal colors.

It would be important to determine precisely which characteristics of the reflectance spectra modulate singularities. Once we know this, we can answer two important question. Once we can characterize the reflectances according to the singularities they produce, we can investigate how these characteristic of the reflectances are related to perceived attributes of color, such as perceived chroma, hue, lightness, variability of colors and color constancy. The perceptual correlates of singularities may give insight into how the properties reflected by singularities are translated into the perception of a human observer.

Moreover, the visual system and color categories might be mainly determined by the natural visual environment human observers experience. Hence, the question arises whether the characteristics of the reflectances that link singularities to focal colors, such as in the case of Munsell chips, also occur in with reflectances in our natural visual environment. Such reflectances are mainly determined by natural pigments and filtering through layers of other material, e.g. cellulose filtering light reflected by chlorophyll. The question is whether these pigments have those particular reflectance properties that produce singularities, which are related to focal colors and color categories. In this case, focal colors would not simply emerge from sensory singularities of all kinds of surfaces under all kinds of illumination changes. Instead, they would be the result of seeing surfaces under changing illuminations as they occur in the visual environment. Hence, color language would be related to objects, with which human observers interact under changing illuminations in the natural environment.

ACKNOWLEDGEMENTS

We thank Alexander V. Terekhov for mathematical advice. This research was supported by a European Research Council funded project (“FEEL”, ref 323674).

REFERENCES

[1] P. Kay and T. Regier, 'Resolving the question of color naming universals'. *Proceedings of the National Academy of Sciences*. 100, p. 9085-9089, (2003).

[2] D.T. Lindsey and A.M. Brown, 'World Color Survey color naming reveals universal motifs and their within-language diversity'. *Proceedings of the National Academy of Sciences USA*. (2009).

[3] D.T. Lindsey and A.M. Brown, 'Universality of color names'. *Proceedings of the National Academy of Sciences*. 103, p. 16608–16613, (2006).

[4] T. Regier, P. Kay, and R.S. Cook, 'Focal colors are universal after all'. *Proceedings of the National Academy of Sciences*. 102, p. 8386–8391, (2005).

[5] M.A. Webster, et al., 'Variations in normal color vision. III. Unique hues in Indian and United States observers'. *Journal of the Optical Society of America A*. 19, p. 1951-62, (2002).

[6] P. Kay and T. Regier, 'Language, thought and color: recent developments'. *Trends in Cognitive Sciences*. 10, p. 51-54, (2006).

[7] C. Witzel and K.R. Gegenfurtner, 'Categorical sensitivity to color differences'. *Journal of vision*. 13, (2013).

[8] K.R. Gegenfurtner and D.C. Kiper, 'Color Vision'. *Annual Review of Neuroscience*. 26, p. 181-206, (2003).

[9] D.L. Philipona and J.K. O'Regan, 'Color naming, unique hues, and hue cancellation predicted from singularities in reflection properties'. *Visual Neuroscience*. 23, p. 331-9, (2006).

[10] J. Vazquez-Corral, et al., 'A new spectrally sharpened sensor basis to predict color naming, unique hues, and hue cancellation'. *Journal of vision*. 12, p. 7, (2012).

[11] J. Romero, A. GarciaBeltran, and J. HernandezAndres, 'Linear bases for representation of natural and artificial illuminants'. *Journal of the Optical Society of America a-Optics Image Science and Vision*. 14, p. 1007-1014, (1997).

[12] C.C. Chiao, T.W. Cronin, and D. Osorio, 'Color signals in natural scenes: characteristics of reflectance spectra and effects of natural illuminants'. *Journal of the Optical Society of America. A, Optics, image science, and vision*. 17, p. 218-24, (2000).

[13] D.B. Judd, et al., 'Spectral Distribution of Typical Daylight as a Function of Correlated Color Temperature'. *J. Opt. Soc. Am.* 54, p. 1031-1036, (1964).

[14] W.S. Stiles and J.M. Burch, 'NPL colour-matching investigation: Final report'. *Optica Acta*. 6, p. 1–26, (1959).

[15] V.C. Smith and J. Pokorny, 'Spectral sensitivity of the foveal cone photopigments between 400 and 500 nm.'. *Vision Research*. 15(2), p. 161, (1975).

[16] A. Stockman and L.T. Sharpe, 'The spectral sensitivities of the middle- and long-wavelength-sensitive cones derived from measurements in observers of known genotype'. *Vision Research*. 40, p. 1711-37, (2000).

[17] J.P.S. Parkkinen, J. Hallikainen, and T. Jaaskelainen, 'Characteristic Spectra of Munsell Colors'. *Journal of the Optical Society of America a-Optics Image Science and Vision*. 6, p. 318-322, (1989).

[18] Munsell Color Services, *The Munsell Book of Color - Glossy Collection*. 2007, Grandville, MI: x-rite.

[19] J.J. Koenderink, 'The prior statistics of object colors'. *Journal of the Optical Society of America A*. 27, p. 206-217, (2010).

[20] G.A. Collier, 'Review of "Basic Color Terms: Their Universality and Evolution"'. *Language*. 49, p. 245-248, (1973).

[21] T. Regier, P. Kay, and N. Khetarpal, 'Color naming reflects optimal partitions of color space'. *Proceedings of the National Academy of Sciences USA*. 104, p. 1436-1441, (2007).

[22] J.B. Cohen and W.E. Kappauf, 'Metameric color stimuli, fundamental metamers, and Wyszecki's metameric blacks'. *Am J Psychol*. 95, p. 537-64, (1982).

[23] C. Witzel and A. Franklin, 'Do focal colors look particularly "colorful"?'. *Journal of the Optical Society of America A*. (in press).

[24] C. Witzel, J. Maule, and A. Franklin, 'Focal colors as perceptual anchors of color categories'. *Journal of Vision*. VSS2013 abstracts, (2013).